AIMS Mathematics, 10(1): 1384–1406.
DOI:10.3934/math.2025064
Received: 25 October 2024
Revised: 15 January 2025
Accepted: 16 January 2025
Published: 21 January 2025

https://www.aimspress.com/journal/Math

Research article

Multi-scale Hochschild spectral analysis on graph data

Yunan He[1] **and Jian Liu**[1,2,*]

[1] Mathematical Science Research Center, Chongqing University of Technology, Chongqing 400054, China

[2] Department of Mathematics, Michigan State University, MI 48824, USA

* **Correspondence:** Email: liujian2@mail.nankai.edu.cn.

Abstract: Topological data analysis (TDA) has experienced significant advancements with the integration of various advanced mathematical tools. While traditional TDA has primarily focused on point cloud data, there is a growing emphasis on the analysis of graph data. In this work, we proposed a spectral analysis method for digraph data, grounded in the theory of Hochschild cohomology. To enable efficient computation and practical application of Hochschild spectral analysis, we introduced the concept of truncated path algebras, along with key mathematical results that support the computation of the Hochschild Laplacian. Our study established key mathematical results, including a relationship between Hochschild Betti numbers and the Euler characteristic of digraphs, as well as efficient representations of Hochschild Laplacian matrices. These innovations enabled us to extract multiscale topological and geometric features from graph data. We demonstrated the effectiveness of our method by analyzing the molecular structures of common drugs, such as ibuprofen and aspirin, producing visualized Hochschild feature curves that capture intricate topological properties. This work provides a novel perspective on digraph analysis and offers practical tools for topological data analysis in molecular and broader scientific applications.

Keywords: topological data analysis; Hochschild cohomology; Hochschild Laplacian; multi-scale; spectral analysis
Mathematics Subject Classification: 05C20, 55N31, 62R40

1. Introduction

Topological data analysis (TDA), as a relatively new method, has gained increasing attention across various fields. The key tool in TDA is persistent homology, introduced by G. Carlsson, H. Edelsbrunner, and others [6, 18]. The main idea of persistent homology is to extract multi-scale topological features that capture the geometric shape and topological structures of data. Persistent

homology has increasingly found success in fields such as molecular biology [4, 30], materials science [22, 23], image science [8, 20], and artificial intelligence [15, 28].

In recent years, with the rapid development of TDA, many advanced topological theories have been applied to this field. These methods include cohomology rings [16], de Rham-Hodge theory [13], Steenrod algebra [27], and others, which have enriched and expanded the scope of topological data analysis. Overall, the development of TDA has progressed across three main areas: topological objects, topological persistence, and topological features. In terms of topological objects, simplicial complex models such as Vietoris-Rips complexes and Čech complexes are no longer sufficient for broader applications, as they typically handle point cloud data but struggle with graph data. As a result, TDA based on the topological theories like embedded homology of hypergraphs [26], path homology of digraphs [14], and hyperdigraph homology [12] has emerged. In terms of topological persistence, new theories have been developed, including multiparameter persistence [9, 10], zigzag persistence [7], and Cayley-persistence algebra [3]. Regarding topological features, in addition to the aforementioned theories, other forms of persistent homology have been introduced, such as persistent intersection homology [2] and persistent interaction homology [24]. The persistent Laplacian, first introduced by Guo-Wei Wei and his coauthors [13, 29], marks an important advancement in topological data analysis. It has since been widely applied in molecular biology, proving effective in capturing the complex structural and functional properties of biomolecules.

Hochschild homology was initially introduced by Gerhard Hochschild [21] for studying the cohomology of associative algebras. Over time, it has been developed as a tool for investigating topological invariants of algebraic structures such as rings, Hopf algebras, Lie algebras, and more. Today, Hochschild homology serves as a fundamental concept in algebraic topology and algebraic geometry, providing insights into the internal structure and symmetries of these algebraic objects. Given a quiver, the path algebra can be constructed in a standard way, allowing us to define Hochschild homology on this path algebra, referred to as the path algebra of the quiver [17]. In particular, Hochschild homology can be defined on digraphs. In [5], the authors introduced persistent Hochschild homology using connectivity digraphs. Inspired by the above work, in this paper, we develop a multiscale Hochschild spectral analysis on graph data.

Traditional simplicial complexes struggle to capture directed edges and multiscale topological features, creating a gap in the application of TDA to directed graph data, which are increasingly common in fields like molecular biology and network science. Motivated by these challenges, we develop a spectral analysis framework for digraphs using Hochschild cohomology. This approach not only addresses the computational inefficiencies of infinite-dimensional path algebras but also integrates harmonic and non-harmonic information to provide a richer characterization of graph data.

In this paper, we introduce the Hochschild Laplacian, and propose a multiscale Hochschild spectral analysis on digraphs. Hochschild cohomology offers a new perspective for analyzing digraph data; however, homological information alone is often insufficient for fully characterizing the structure of graph data. To address this, we introduce the spectral information of the Hochschild Laplacian to study the multiscale topological features and geometric properties of digraphs. The Hochschild Laplacian is of particular interest because its harmonic component contains Hochschild cohomology information, while its non-harmonic component encodes the geometric information of digraphs in a metric space. One challenge in computing and applying the Hochschild Laplacian is that the path algebra is often infinite-dimensional. Instead of adopting the connectivity digraph construction from [5] to circumvent

this issue, we consider the truncated path algebra, which is more computationally feasible and whose Hochschild Laplacian construction also encompasses information from the traditional graph Laplacian. Additionally, some mathematical results in this paper simplify the computation of certain Hochschild Laplacian matrices. For specific molecules, we utilize the distances between atoms to construct multiscale information, enabling the computation of their topological features and geometric properties across scales. We demonstrate the application of this method on common drug molecules, such as ibuprofen and aspirin, yielding rich topological and geometric insights. Compared to existing methods, our approach combines computational efficiency with the ability to capture both harmonic and non-harmonic features of digraphs, including higher-order topological and geometric information. These advantages make it particularly suitable for analyzing complex graph structures, such as molecular data.

The paper is organized as follows. In the next section, we review some fundamental concepts and results related to Hochschild cohomology and path algebras. Section 3 outlines our main methods and relevant mathematical results, including truncated path algebras, the Hochschild Laplacian, and multiscale Hochschild spectra. In Section 4, we apply the Hochschild spectral analysis to drug molecules. The final section provides a summary of the paper.

2. Hochschild cohomology and path algebra

In this section, we will review the basic concepts of Hochschild cohomology and path algebras. From now on, $\mathbb{K}$ is assumed to be a field of characteristic zero.

2.1. Hochschild cohomology

Let A be an associative algebra over $\mathbb{K}$. From now on, unless otherwise specified, the tensor product $\otimes$ denotes $\otimes_{\mathbb{K}}$, and $\mathrm{Hom}(-,-)$ denotes $\mathrm{Hom}_{\mathbb{K}}(-,-)$ for simplicity. Let $A^{\otimes n} = \underbrace{A \otimes \cdots \otimes A}_{n}$. For an A-bimodule M, let $C^n(A,M) = \mathrm{Hom}(A^{\otimes n}, M)$. Then, we have homomorphisms $d^i : C^n(A,M) \to C^{n+1}(A,M)$ given by

$$\begin{aligned}(d^0 m)(a) &= am - ma,\\ (d^n f)(a_1 \otimes \cdots \otimes a_{n+1}) &= a_1 f(a_2 \otimes \cdots \otimes a_{n+1}) + \sum_{i=1}^{n} (-1)^i f(a_1 \otimes \cdots \otimes a_i a_{i+1} \otimes \cdots \otimes a_{n+1})\\ &\quad -(-1)^n f(a_1 \otimes \cdots \otimes a_n) a_{n+1}.\end{aligned}$$

It can be proved that $d^{n+1}d^n = 0$ for $n \geq 0$. The Hochschild complex $C^*(A,M)$ is the cochain complex

$$0 \longrightarrow M \xrightarrow{d^0} C^1(A,M) \xrightarrow{d^1} \cdots \xrightarrow{d^{n-2}} C^{n-1}(A,M) \xrightarrow{d^{n-1}} C^n(A,M) \xrightarrow{d^n} \cdots .$$

The differential d_n is called the Hochschild differential. Let us denote $Z^n(A,M) = \ker d^n$ and $B^n(A,M) = \mathrm{im}\, d^{n-1}$. Then, we have $B^n(A,M) \subseteq Z^n(A,M)$.

Definition 2.1. *The Hochschild cohomology of A with coefficients in M is defined by*

$$HH^n(A,M) = Z^n(A,M)/B^n(A,M), \quad n \geq 0.$$

In particular, we denote $HH^n(A) = HH^n(A, A)$. The rank of the Hochschild cohomology, denoted by $\beta_H^n(A, M) = \text{rank}_{\mathbb{K}} HH^n(A, M)$ for $n \geq 0$, is called the *Hochschild Betti number*. The following lemma is obtained by a straightforward calculation.

Lemma 2.1. *(i)* $HH^0(A, M) = Z_A(M) = \{x \in M | xa = ax \text{ for any } a \in A\}$.

(ii) $Z^1(A, M) = \text{Der}_A(M) = \{\delta \in \text{Hom}(A, M) | \delta(ab) = \delta(a)b + a\delta(b) \text{ for any } a, b \in A\}$.

Example 2.1. *(i) Let* $A = \mathbb{K}[x]$ *be a one-variable polynomial algebra. Then, the Hochschild cohomology of A is* $HH^n(A) \cong \begin{cases} A, & n = 0, 1; \\ 0, & \text{otherwise.} \end{cases}$

(ii) Consider the truncated polynomial algebra $A = \mathbb{K}[x]/(x^k)$ *for* $k > 1$. *Then, we have the Hochschild cohomology* $HH^n(A) = \begin{cases} A, & n = 0; \\ (x)A, & n > 0 \text{ is even;} \\ A/(x^{k-1}), & n > 0 \text{ is odd.} \end{cases}$

The Hochschild cohomology generators offer critical insights into the algebraic and geometric structures of a given algebra. In dimension 0, the Hochschild cohomology (HH^0) corresponds to the center of the algebra A, consisting of elements that commute with every other element. This reflects the algebra's symmetries. Geometrically, HH^0 represents zero-dimensional topological features of the associated manifold, such as fixed points or isolated structures that remain invariant under transformations. In dimension 1, the Hochschild cohomology (HH^1) captures the infinitesimal deformations of the algebra A, describing how the algebra changes under small perturbations or parameter adjustments. Geometrically, HH^1 corresponds to vector fields on the manifold, which represent directional flows or infinitesimal symmetries, illustrating how the structure can be locally deformed. For higher dimensions ($HH^n, n \geq 2$), the generators encode more complex interactions within the algebra, such as multi-variable deformations and nested relationships among elements of A. Geometrically, these cohomology classes generalize the concepts of vector fields and symmetries to higher dimensions, representing multi-directional flows, higher-order deformations, or constraints within the manifold's structure.

2.2. Hochschild cohomology of path algebra

A *directed graph* (digraph) $G = (V, E)$ is a finite nonempty set V, called the vertex set, equipped with an edge set $E \subseteq V \times V$. For an edge $e = (v, v') \in E$, we denote $s(e) = v$ as the source of e, and $t(e) = v'$ as the target of e. A *path* on G is a sequence of $v_0v_1 \cdots v_k$ such that $(v_{i-1}, v_i) \in E$ for $i = 1, 2, \ldots, k$. The length of a path $\gamma = v_0v_1 \cdots v_k$ is defined as $\ell(\gamma) = k$. The vertices can be regarded as trivial paths of length zero.

Let $\mathbb{K}$ be a field, and let G be a digraph. The *path algebra* $\Omega(G)$ of G is the $\mathbb{K}$-linear space generated by all the paths on G, with the product defined as follows:

$$(v_0v_1 \cdots v_k) * (w_0w_1 \cdots w_l) = \begin{cases} v_0v_1 \cdots v_kw_1 \cdots w_l, & \text{if } v_k = w_0; \\ 0, & \text{otherwise.} \end{cases}$$

Note that $\ell((v_0v_1 \cdots v_k) * (w_0w_1 \cdots w_l)) = \begin{cases} k + l, & v_k = w_0; \\ 0, & \text{otherwise.} \end{cases}$ Hence, $\Omega(G)$ is a graded algebra, and we can express it as $\Omega(G) = \bigoplus_{i \geq 0} \Omega_i(G)$. A *cycle* in G is a path $v_0v_1 \cdots v_k$ of $k \geq 1$ such that $v_0 = v_k$.

Proposition 2.2. *Let $G = (V, E)$ be a digraph. Then, $\Omega(G)$ is a finite-dimensional associative algebra if and only if G has no cycles.*

Proof. If G has no cycles, then each path is of the form $\gamma = v_0v_1 \cdots v_k$ for distinct vertices $v_0, v_1, \ldots, v_k$ in V. Since V is finite, the length of γ is at most $N - 1$, where $N = |V|$ denotes the number of elements in V. The number of directed paths of length no greater than $N - 1$ is less than $(N + 1)^N$. Therefore, we have $\dim \Omega(G) < (N + 1)^N$.

On the other hand, if G contains a cycle $\gamma = v_0v_1 \cdots v_k$ for some $k \geq 1$, then there exists a family of paths $\{\gamma^r\}_{r\geq 1}$. Since $\gamma^r \neq 0$ for any $r \geq 1$ and $\ell(\gamma^r) = kr$, it follows that there are infinitely many paths in $\Omega(G)$. Thus, $\Omega(G)$ is not a finite-dimensional algebra. □

Example 2.2. *Let $G = (V, E)$ be a digraph given by $V = \{v\}$ and $E = \{(v, v)\}$. Then, $\Omega(G) = \mathbb{K}[x]$ is a polynomial algebra. The corresponding Hochschild cohomology is given by $HH^k(\Omega(G)) = \begin{cases} \mathbb{K}[x], & k = 0, 1; \\ 0, & \text{otherwise.} \end{cases}$ Thus, the Hochschild cohomology $HH^k(\Omega(G))$ is an infinite dimensional algebra.*

Example 2.3. *Consider the digraph $G = (V, E)$ given by*

$$V = \{v_0, v_1, v_2\}, \quad E = \{(v_0, v_1), (v_0, v_2), (v_1, v_2)\}.$$

The corresponding path algebra $\Omega(G)$ is a $\mathbb{K}$-linear space generated by v_0, v_1, v_2, and v_0v_1, v_0v_2, v_1v_2. The identity element is $v_0 + v_1 + v_2$. The nontrivial product is given by

$$\begin{aligned} v_0 * v_0v_1 &= v_0v_1 * v_1 = v_0v_1, \\ v_0 * v_0v_2 &= v_0v_2 * v_2 = v_0v_2, \\ v_1 * v_1v_2 &= v_1v_2 * v_2 = v_1v_2, \\ v_0v_1 * v_1v_2 &= v_0v_1v_2. \end{aligned}$$

By a direct computation, we have

$$HH^0(\Omega(G)) = \mathbb{K}\{v_0 + v_1 + v_2\}.$$

Let $C^n(\Omega(G)) = C^n(\Omega(G), \Omega(G))$. We have the following cochain complex:

$$0 \longrightarrow \Omega(G) \xrightarrow{d^0} C^1(\Omega(G)) \xrightarrow{d^1} C^2(\Omega(G)) \xrightarrow{d^2} \cdots.$$

Let us compute

$$\ker d^1 = \{\delta \in \mathrm{Hom}(\Omega(G), \Omega(G)) | \delta(ab) = \delta(a)b + a\delta(b) \text{ for any } a, b \in \Omega(G)\}.$$

By considering the equation $\delta(v_s * v_t) = \delta(v_s) * v_t + v_s * \delta(v_t)$, we have

$$\begin{aligned} \delta(v_0) = &\quad a_1v_0v_1 + a_2v_0v_2 + b_1v_0v_1v_2, \\ \delta(v_1) = &\quad -a_1v_0v_1 + a_3v_1v_2, \\ \delta(v_2) = &\quad -a_2v_0v_2 - a_3v_1v_2 - b_1v_0v_1v_2, \end{aligned}$$

where $a_1, a_2, a_3, b_1 \in \mathbb{K}$. Similarly, by using the Leibniz rule on $\delta(v_s * v_0v_1)$ and $\delta(v_0v_1 * v_t)$, we have

$$\begin{aligned}\delta(v_0v_1) = &\quad c_1v_0v_1 + a_3v_0v_1v_2,\\ \delta(v_0v_2) = &\quad c_2v_0v_2 + b_2v_0v_1v_2,\\ \delta(v_1v_2) = &\quad c_3v_1v_2 - a_1v_0v_1v_2,\end{aligned}$$

where $c_1, c_2, c_3, b_2 \in \mathbb{K}$. Besides, we have $\delta(v_0v_1v_2) = (c_1 + c_3)v_0v_1v_2$. For path γ_1, γ_1 on G, let us denote $\gamma_1 \cdot \gamma_2^\sharp : \Omega(G) \to \Omega(G)$ as follows:

$$(\gamma_1 \cdot \gamma_2^\sharp)(\gamma) = \begin{cases} \gamma_1, & \gamma = \gamma_2;\\ 0, & \text{otherwise.}\end{cases}$$

Then, $Z^1(\Omega(G)) = \ker d^1$ is a $\mathbb{K}$-linear space generated by the elements

$$\begin{aligned}&v_0v_1 \cdot (v_0^\sharp - v_1^\sharp) + v_0v_1v_2 \cdot (v_1v_2)^\sharp, \quad v_0v_2 \cdot (v_0^\sharp - v_2^\sharp), \quad v_1v_2 \cdot (v_1^\sharp - v_2^\sharp) + v_0v_1v_2 \cdot (v_0v_1)^\sharp,\\ &v_0v_1v_2 \cdot (v_0^\sharp - v_2^\sharp), \quad v_0v_1 \cdot (v_0v_1)^\sharp + v_0v_1v_2 \cdot (v_0v_1v_2)^\sharp, \quad v_0v_2 \cdot (v_0v_2)^\sharp,\\ &v_1v_2 \cdot (v_1v_2)^\sharp + v_0v_1v_2 \cdot (v_0v_1v_2)^\sharp, \quad v_0v_1v_2 \cdot (v_0v_2)^\sharp.\end{aligned}$$

On the other hand, a step-by-step calculation shows that $\operatorname{im} d^0$ is generated by

$$\begin{aligned}&v_0v_1 \cdot (v_0^\sharp - v_1^\sharp) + v_0v_1v_2 \cdot (v_1v_2)^\sharp, \quad v_0v_2 \cdot (v_0^\sharp - v_2^\sharp), \quad v_1v_2 \cdot (v_1^\sharp - v_2^\sharp) + v_0v_1v_2 \cdot (v_0v_1)^\sharp,\\ &v_0v_1v_2 \cdot (v_0^\sharp - v_2^\sharp), \quad v_0v_1 \cdot (v_0v_1)^\sharp + v_0v_1v_2 \cdot (v_0v_1v_2)^\sharp, v_1v_2 \cdot (v_1v_2)^\sharp + v_0v_1v_2 \cdot (v_0v_1v_2)^\sharp.\end{aligned}$$

It follows that

$$HH^1(\Omega(G)) \cong \mathbb{K}\{v_0v_2 \cdot (v_0v_2)^\sharp, v_0v_1v_2 \cdot (v_0v_2)^\sharp\}.$$

Let K be a simplicial complex. The subdivision $\mathrm{sd}(K)$ of K is the simplicial complex whose p-simplices are of the form $\sigma_0\sigma_1 \cdots \sigma_p$, where $\sigma_0 \subset \sigma_1 \subset \cdots \subset \sigma_p$ and $\sigma_0, \sigma_1, \ldots, \sigma_p \in K$. We can regard $\mathrm{sd}(K)$ as a digraph, whose vertex set is the set of simplices of K, and whose edge set consists of pairs (σ, τ) where $\tau \subseteq \sigma$. Let $\Lambda(K)$ denote the path algebra associated with the digraph obtained from $\mathrm{sd}(K)$. It is a classical result that the Hochschild cohomology of $\Lambda(K)$ coincides with the simplicial cohomology of K.

Theorem 2.3. *[19]* $HH^*(\Lambda(K)) \cong H^*(K)$.

3. Hochschild Laplacians on truncated algebra

Digraphs are common mathematical objects and data structures. A natural idea presented in this paper is to use Hochschild homology information as a topological feature of digraphs for data analysis. As mentioned in Proposition 2.2 in the previous section, the path algebra of a digraph with directed cycles is infinite-dimensional, which is unsuitable for computation and practical applications. Therefore, we consider working with truncated path algebras to obtain Hochschild homology and spectral information for data analysis. In this section, we will establish the theoretical foundation for Hochschild homotopy and Hochschild Laplacians based on truncated path algebras.

3.1. Truncated path algebra

Let G be a digraph. The *N-truncated path algebra* $\Omega_{\leq N}(G)$ of G is the $\mathbb{K}$-linear space generated by all paths of length not larger than N. The product of two paths $\gamma \cdot \gamma'$ in $\Omega_{\leq N}(G)$ coincides with the product in $\Omega(G)$ if $\ell(\gamma) + \ell(\gamma') \leq N$, and $\gamma \cdot \gamma' = 0$ if $\ell(\gamma) + \ell(\gamma') > N$. A digraph is *simple* if it has no loops or parallel edges. From now on, for the sake of simplicity, all the digraphs considered are assumed to be simple.

Lemma 3.1. *Let $A = \mathbb{K}\{x_1, \ldots, x_r\}$ be a $\mathbb{K}$-algebra with the multiplication given by*

$$x_i x_j = \begin{cases} x_i, & x_i = x_j; \\ 0, & \textit{otherwise.} \end{cases}$$

Then, we have

$$HH^n(A) = \begin{cases} A, & n = 0; \\ 0, & n \geq 1. \end{cases}$$

Proof. Let A^{op} be the opposite algebra of A, and let $A^e = A \otimes A^{op}$ be the enveloping algebra of A. Then, we have a free resolution of A as follows:

$$\cdots \xrightarrow{\eta} A^e \xrightarrow{\lambda} A^e \xrightarrow{\eta} A^e \xrightarrow{\lambda} A^e \xrightarrow{\mu} A \longrightarrow 0.$$

Here, $\mu(x \otimes y) = xy$, $\lambda(x_i \otimes x_j) = \begin{cases} x_i \otimes x_j, & i \neq j; \\ 0, & i = j, \end{cases}$ and $\eta(x_i \otimes x_j) = \begin{cases} x_i \otimes x_j, & i = j; \\ 0, & i \neq j. \end{cases}$ By applying the left exact functor $\mathrm{Hom}_{A^e}(-, A)$, we have the sequence

$$0 \longrightarrow \mathrm{Hom}_{A^e}(A^e, A) \xrightarrow{\lambda^*} \mathrm{Hom}_{A^e}(A^e, A) \xrightarrow{\eta^*} \mathrm{Hom}_{A^e}(A^e, A) \xrightarrow{\lambda^*} \cdots$$

$$0 \longrightarrow A \xrightarrow{\lambda^*} A \xrightarrow{\eta^*} A \xrightarrow{\lambda^*} A \xrightarrow{\eta^*} \cdots,$$

where $\lambda^* = 0$ and $\eta^* = \mathrm{id}$. By the well-known isomorphism $HH^n(A, M) = \mathrm{Ext}^n_{A^e}(A, M)$, we have the desired result. □

Proposition 3.2. *Let $G = (V, E)$ be a digraph. Then, we have*

$$HH^n(\Omega_{\leq 0}(G)) = \begin{cases} \Omega_{\leq 0}(G), & n = 0; \\ 0, & n \geq 1. \end{cases}$$

Proof. It is a direct result of Lemma 3.1. □

Theorem 3.3. *Let G be a digraph. Then, we have*

$$\beta^0_H(\Omega_{\leq 1}(G)) = 1, \quad \beta^1_H(\Omega_{\leq 1}(G)) = 1 - \chi(G).$$

Here, $\chi(G)$ denotes the Euler characteristic of G as a 1-dimensional simplicial complex.

Proof. By definition, we have

$$HH^0(\Omega_{\leq 1}(G)) = Z(\Omega_{\leq 1}(G)) = \mathbb{K}\{\sum_{v\in V} v\}.$$

Let $V = \{v_1, v_2, \ldots, v_k\}$ and $E = \{e_1, e_1, \ldots, v_l\}$. Consider the following cochain complex:

$$0 \longrightarrow \Omega_{\leq 1}(G) \xrightarrow{d^0} C^1(\Omega_{\leq 1}(G)) \xrightarrow{d^1} C^2(\Omega_{\leq 1}(G)) \xrightarrow{d^2} \cdots .$$

Note that $\ker d^1 = \mathrm{Der}(\Omega_{\leq 1}(G))$. For any $\delta \in \ker d^1$, we have $\delta(ab) = \delta(a)b + a\delta(b)$ for $a, b \in \Omega_{\leq 1}(G)$. By applying $\delta(v_s * v_t) = \delta(v_s) * v_t + v_s * \delta(v_t)$ for the case $s = t$, we obtain that

$$\delta(v_s) = \sum_{e_j} a_{s,j} e_j, \quad a_{s,j} \in \mathbb{K},$$

where the sum $\sum$ runs over all edges of the form $(v_s, -)$ or $(-, v_s)$. Here, we use the edge e to denote a path of length 1 for simplicity. For $s \neq t$, if e_j is of the form (v_s, v_t) or (v_t, v_s), we obtain

$$a_{s,j} + a_{t,j} = 0.$$

Thus, the basis of δ on $v_1, v_2, \ldots, v_k$ is given by $\{v_s v_t \cdot (v_s - v_t)^\sharp\}_{s,t}$, where $v_s v_t$ or $v_t v_s$ is an edge in E. Note that

$$\delta(v_r v_s * v_t) = \delta(v_r v_s) * v_t + v_r v_s * \delta(v_t) = \delta(v_r v_s) * v_t.$$

Assume that $\delta(v_r v_s) = \sum\limits_{i=1}^{k} b_i v_i + \sum\limits_{j=1}^{l} c_j e_j$ for some $b_i, c_j \in \mathbb{K}$. We have

$$\sum_{i=1}^{k} b_i v_i + \sum_{j=1}^{l} c_j e_j = b_s v_s + \sum_{j=1}^{l} c_j e_j v_s.$$

It follows that $b_i = 0$ for $i \neq s$. Similarly, by applying the Leibniz rule on $v_r * v_s v_t$, we obtain $b_i = 0$ for $i \neq r$. Since G is simple, we have $r \neq s$. It follows that $b_i = 0$ for any i. Note that $\sum\limits_{j=1}^{l} c_j e_j = \sum\limits_{j=1}^{l} c_j e_j v_s$ and $\sum\limits_{j=1}^{l} c_j e_j = v_r \sum\limits_{j=1}^{l} c_j e_j$, and we obtain that

$$\delta(v_r v_s) = c_{rs} v_r v_s, \quad c_{rs} \in \mathbb{K}.$$

Let S_v denote the set of edges of the form $(v, -)$ or $(-, v)$. Hence, the linear space $\ker d^1$ is generated by $\{v_s v_t \cdot (v_s - v_t)^\sharp\}_{s,t}$ for edges $v_s v_t$ or $v_t v_s$ and

$$e_1 \cdot e_1^\sharp, e_2 \cdot e_2^\sharp, \ldots, e_l \cdot e_l^\sharp.$$

Thus, we have

$$\dim \ker d^1 = (\sum_{i=1}^{k} d_i) - l + l = 2l.$$

Here, d_i denotes the degree of the vertex v_i, meaning the number of edges connected to v_i. On the other hand,

$$\dim \operatorname{im} d^0 = \dim \Omega_{\leq 1}(G) - \dim \ker d^0 = k + l - 1.$$

It follows that

$$\beta^1_H(\Omega_{\leq 1}(G)) = \dim \ker d^1 - \dim \operatorname{im} d^0 = l - k + 1.$$

By the Euler formula, we have $\chi(G) = \beta^0(G) - \beta^1(G) = k - l$. It follows that $\beta^1_H = 1 - \chi(G)$. □

Example 3.1. *Let $G = C_m$ be a digraph with the vertex set and edge set*

$$V = \{v_1, v_2, \ldots, v_m\}, \quad E = \{(v_1, v_2), \ldots, (v_{m-1}, v_m), (v_m, v_1)\}.$$

By Lemma 2.1, one has that

$$HH^0(\Omega_{\leq 1}(G)) = \mathbb{K}\{v_1 + v_2 + \cdots + v_m\}.$$

On the other hand, the space $\ker d^1 = \mathrm{Der}(\Omega_{\leq 1}(G))$ is generated by the elements

$$\begin{aligned} &v_1v_2 \cdot (v_1^\sharp - v_2^\sharp), \ldots, v_{m-1}v_m \cdot (v_{m-1}^\sharp - v_m^\sharp), v_mv_1 \cdot (v_m^\sharp - v_1^\sharp), \\ &v_1v_2 \cdot (v_1v_2)^\sharp, \ldots, v_{m-1}v_m \cdot (v_{m-1}v_m)^\sharp, v_mv_1 \cdot (v_mv_1)^\sharp. \end{aligned}$$

Recall that $d^0 : \Omega_{\leq 1}(G) \to C^1(\Omega_{\leq 1}(G))$ is given by $d^0(a)x = xa - ax$. It follows that

$$d^0(v_r)(x) = \begin{cases} -x, & x = v_rv_{r+1}; \\ x, & x = v_{r-1}v_r; \\ 0, & \text{otherwise.} \end{cases}$$

Here, we make the convention that $v_{-1} = v_m$ and $v_{m+1} = v_1$ for convenience. Moreover, we have

$$d^0(v_rv_{r+1})(x) = \begin{cases} v_rv_{r+1}, & x = v_r; \\ -v_rv_{r+1}, & x = v_{r+1}; \\ 0, & \text{otherwise.} \end{cases}$$

It follows that $\operatorname{im} d^0$ is generated by

$$v_{r-1}v_r \cdot (v_{r-1}v_r)^\sharp - v_rv_{r+1} \cdot (v_rv_{r+1})^\sharp, \quad v_rv_{r+1} \cdot (v_r^\sharp - v_{r+1}^\sharp)$$

for $r = 1, 2, \ldots, m$. Thus, the Hochschild homology is

$$HH^1(\Omega_{\leq 1}(G)) = \mathbb{K}\{[v_1v_2 \cdot (v_1^\sharp - v_2^\sharp)]\}.$$

Here, $[v_1v_2 \cdot (v_1^\sharp - v_2^\sharp)]$ is an equivalent class of the homology generator. The Euler characteristic of a circle is 0. By Theorem 3.3, one has $\beta^1_H(\Omega_{\leq 1}(G)) = 1 - \chi(G) = 1$. This aligns with the result from the above calculations.

3.2. Hochschild Laplacians

In this section, the field $\mathbb{K}$ is taken to be the real number field $\mathbb{R}$.

Let V and W be inner product spaces. Then the tensor product $V \otimes W$ is also an inner product space, with the inner product defined as:

$$\langle v_1 \otimes w_1, v_2 \otimes w_2 \rangle_{V\otimes W} = \langle v_1, v_2 \rangle_V \langle w_1, w_2 \rangle_W,$$

where $v_1, v_2 \in V$ and $w_1, w_2 \in W$. For any map $f \in \mathrm{Hom}(V, W)$, the adjoint map f^* of f is defined as

$$\langle f(v), w \rangle = \langle v, f^*(w) \rangle, \quad \text{for any } v \in V, w \in W.$$

Then, the space $\mathrm{Hom}(V, W)$ is an inner product space, with the inner product, known as the Frobenius inner product, given by

$$\langle f, g \rangle_{\mathrm{Hom}(V,W)} = \mathrm{tr}(f^* g) = \mathrm{tr}(g f^*),$$

where $f, g \in \mathrm{Hom}(V, W)$ and tr denotes the trace of linear transformations.

From now on, for simplicity, all inner products will be denoted by $\langle -, - \rangle$. Let A be a finite dimensional algebra over $\mathbb{R}$. Suppose A is an inner product space with the inner product structure $\langle -, - \rangle$. Then, $A^{\otimes n}$ and $C^n(A)$ are also inner product spaces.

We have a Hochschild complex $C^*(A)$ as follows:

$$0 \longrightarrow A \xrightarrow{d^0} C^1(A) \xrightarrow{d^1} \cdots \xrightarrow{d^{n-2}} C^{n-1}(A) \xrightarrow{d^{n-1}} C^n(A) \xrightarrow{d^n} \cdots .$$

The n-th *Hochschild Laplacian* of A is

$$\Delta^n = (d^n)^* \circ d^n + d^{n-1} \circ (d^{n-1})^*, \quad n \geq 0.$$

Specifically, for $n = 0$, we have $\Delta^0 = (d^0)^* \circ d^0$. It is clear that Δ^n is a self-adjoint and non-negative operator.

Let G be a digraph. The truncated algebra $\Omega_{\leq N}(G)$ is a finite dimensional algebra. We endow $\Omega_{\leq N}(G)$ with the inner product structure defined as follows:

$$\langle \gamma, \gamma' \rangle = \begin{cases} 1, & \gamma = \gamma'; \\ 0, & \text{otherwise.} \end{cases}$$

Thus, we can obtain the Hochschild Laplacian $\Delta_N^n : C^n(\Omega_{\leq N}(G)) \to C^n(\Omega_{\leq N}(G))$ of truncated algebra $\Omega_{\leq N}(G)$.

Theorem 3.4. *Let G be a digraph. Then, we have*

$$HH^n(\Omega_{\leq N}(G)) \cong \ker \Delta_N^n, \quad n \geq 0.$$

Proof. Consider the cochain complex

$$0 \longrightarrow \Omega_{\leq N}(G) \xrightarrow{d^0} C^1(\Omega_{\leq N}(G)) \xrightarrow{d^1} \cdots \xrightarrow{d^{n-1}} C^n(\Omega_{\leq N}(G)) \xrightarrow{d^n} \cdots .$$

It follows that $\ker \Delta_N^n = \ker d^n \cap \ker(d^{n-1})^*$. Note that the inclusion $\iota : (\ker \Delta_N^*, 0) \hookrightarrow C^*(\Omega_{\leq N}(G)$ is a morphism of cochain complexes, which induces a $\mathbb{K}$-linear map $\iota^* : \ker \Delta_N^* \to HH^*(\Omega_{\leq N}(G))$. Here, $\ker \Delta_N^* = \bigoplus_{n\geq 0} \Delta_N^n$. If $\iota(x)$ is a coboundary in $C^*(\Omega_{\leq N}(G)$ for $x \in \ker \Delta_N^n$, we can write $x = d^{n-1} z$ for some $z \in C^{n-1}(\Omega_{\leq N}(G)$. But $x \in \ker d^n$, so it follows that $x = 0$. Thus the map ι^* is an injection. On the other hand, for any cocycle y in $C^n(\Omega_{\leq N}(G))$, by [25, Proposition 3.1], we can write $y = y_0 + d^{n-1} y_1$ for $y_0 \in \ker \Delta_N^n$ and $y_1 \in C^{n-1}(\Omega_{\leq N}(G))$. It follows that $\iota^*([y_0]) = [y]$. Thus the map ι^* is a surjection. The desired result follows. □

3.3. The representation matrix of the Hochschild Laplacian

The Laplacian matrix of a graph is a fundamental tool for analyzing graph structure, connectivity, and spectral clustering, with its eigenvalues and eigenvectors revealing essential properties of the graph. It also has broad applications in signal processing, random walks, and optimization problems, making it a crucial instrument for studying networks and graph data, as illustrated in recent studies [1]. Note that a digraph G can be regarded as a graph if the direction of its edges is ignored. The corresponding Laplacian matrix for this graph is referred to as the *symmetric Laplacian* of G.

Let G be a digraph. Let $V = \{v_1, v_2, \ldots, v_k\}$ be the set of vertices in G, and let $E = \{e_1, e_2, \ldots, e_l\}$. We denote $\mathbf{v} = (v_1, v_2, \ldots, v_k)^T$ and $\mathbf{e} = (e_1, e_2, \ldots, e_l)^T$. Besides, let $\mathbf{v}^\sharp = (v_1^\sharp, v_2^\sharp, \ldots, v_k^\sharp)^T$ and $\mathbf{e}^\sharp = (e_1^\sharp, e_2^\sharp, \ldots, e_l^\sharp)^T$. Then the representation matrix D_0 of the differential $d^0 : C^0(\Omega_{\leq 1}(G)) \to C^1(\Omega_{\leq 1}(G))$ is given by

$$d^0 \begin{pmatrix} \mathbf{v} \\ \mathbf{e} \end{pmatrix} = D_0 \begin{pmatrix} \mathbf{v} \otimes \mathbf{v}^\sharp \\ \mathbf{v} \otimes \mathbf{e}^\sharp \\ \mathbf{e} \otimes \mathbf{v}^\sharp \\ \mathbf{e} \otimes \mathbf{e}^\sharp \end{pmatrix}.$$

Here, $\mathbf{v} \otimes \mathbf{v}^\sharp = \begin{pmatrix} v_1 \cdot \mathbf{v}^\sharp \\ \vdots \\ v_k \cdot \mathbf{v}^\sharp \end{pmatrix}$, $\mathbf{v} \otimes \mathbf{e}^\sharp = \begin{pmatrix} v_1 \cdot \mathbf{e}^\sharp \\ \vdots \\ v_k \cdot \mathbf{e}^\sharp \end{pmatrix}$, $\mathbf{e} \otimes \mathbf{v}^\sharp = \begin{pmatrix} e_1 \cdot \mathbf{v}^\sharp \\ \vdots \\ e_l \cdot \mathbf{v}^\sharp \end{pmatrix}$, and $\mathbf{e} \otimes \mathbf{e}^\sharp = \begin{pmatrix} e_1 \cdot \mathbf{e}^\sharp \\ \vdots \\ e_l \cdot \mathbf{e}^\sharp \end{pmatrix}$.

Theorem 3.5. *Let $G = (V, E)$ be a digraph. Suppose the symmetrization of G is a simple graph. Then the representation matrix of Δ_1^0 is given by*

$$L_1^0 = \begin{pmatrix} L_G & 0 \\ 0 & 2I_{|E|} \end{pmatrix}.$$

Here, L_G is the symmetric Laplacian matrix of G, and $I_{|E|}$ is the identity matrix of ord $|E|$.

Proof. Similar to Example 3.1, the differential $d^0 : \Omega_{\leq 1}(G) \to C^1(\Omega_{\leq 1}(G))$ is given by

$$d^0(v_r)(x) = \begin{cases} -x, & x = v_r v_s; \\ x, & x = v_s v_r; \\ 0, & \text{otherwise}, \end{cases}$$

and

$$d^0(v_r v_s)(x) = \begin{cases} v_r v_s, & x = v_r; \\ -v_r v_s, & x = v_s; \\ 0, & \text{otherwise}. \end{cases}$$

Hence, the representation matrix D_0 is of the form $\begin{pmatrix} 0 & 0 & 0 & A \\ 0 & 0 & B & 0 \end{pmatrix}$. Here, the matrices A and B are given by

$$d^0\mathbf{v} = A\mathbf{e} \otimes \mathbf{e}^\sharp, \quad d^0\mathbf{e} = B\mathbf{e} \otimes \mathbf{v}^\sharp.$$

Note that the coefficients of $e_r \cdot e_s^\sharp$ in $A\mathbf{e} \otimes \mathbf{e}^\sharp$ are zero. Let us denote $AA^T = (a_{i,j})_{1 \leq i,j \leq k}$. It follows that

$$a_{ij} = \begin{cases} \deg v_i, & i = j; \\ -1, & v_i v_j \text{ or } v_j v_i \text{ is an edge}; \\ 0, & \text{otherwise}. \end{cases}$$

Thus, AA^T is the Laplacian matrix. Similarly, let $BB^T = (b_{i,j})_{1\leq i,j\leq l}$. One can obtain:

$$b_{ij} = \begin{cases} 2, & i = j; \\ 0, & \text{otherwise.} \end{cases}$$

Hence, the matrix BB^T is given by $2I_{|E|}$. □

Remark 3.1. *Let $G = (V, E)$ be a digraph. Recall that the Laplacian matrix of a graph is given by $L = D - M$, where D is the degree matrix, and M is the adjacency matrix of G. Alternatively, the Laplacian can be expressed using the incidence matrix. The incidence matrix $N = (N_{ij})$ is defined as follows:*

$$N_{ij} = \begin{cases} 1, & \text{if } e_j \text{ originates from } v_i, \\ -1, & \text{if } e_j \text{ points to } v_i, \\ 0, & \text{otherwise.} \end{cases}$$

With this definition, the Laplacian matrix can be written as $L = NN^T$.

Let $G = (V, E)$ be a digraph. Define Ω_i as the linear subspace generated by paths of length i. Then, the space $\Omega_{\leq N}(G)$ admits a direct sum decomposition:

$$\Omega_{\leq N}(G) = \bigoplus_{i=0}^{N} \Omega_i(G).$$

Consequently, we have

$$C^1(\Omega_{\leq N}(G)) = \bigoplus_{i,j} \mathrm{Hom}(\Omega_i(G), \Omega_j(G)).$$

This decomposition provides a clearer understanding of the differential d^0.

Lemma 3.6. *Let G be a digraph. The differential $d^0 : \Omega_{\leq N}(G) \to C^1(\Omega_{\leq N}(G))$ has a decomposition $d^0 = \bigoplus_{i=1}^{N} d_i^0$, where $d_i^0 : \Omega_i(G) \to \mathrm{Hom}(\Omega_i(G), \Omega_i(G))$.*

Proof. It can be obtained directly by definition. □

The above decomposition also provides a decomposition of the Hochschild cohomology

$$HH^0(\Omega_{\leq N}(G)) = \bigoplus_{i=1}^{N} HH^{0,i}(\Omega_{\leq N}(G)).$$

Here, $HH^{0,i}(\Omega_{\leq N}(G))$ denotes the subspace of $HH^0(\Omega_{\leq N}(G))$ spanned by the generators derived from the elements of $\Omega_i(G)$. We denote the rank of $HH^{0,i}(\Omega_{\leq N}(G))$ by $\beta_{H,N}^{0,i}$, which is equal to the number of zero eigenvalues of $\Delta_{N,i}^0$.

Proposition 3.7. *Let $G = (V, E)$ be a digraph. The Hochschild Laplacian $\Delta_N^0 : \Omega_{\leq N}(G) \to \Omega_{\leq N}(G)$ has a decomposition $\Delta_N^0 = \bigoplus_{i=1}^{N} \Delta_{N,i}^0$, where $\Delta_{N,i}^0 = (d_i^0)^* d_i^0 : \Omega_i(G) \to \Omega_i(G)$.*

Proof. By Lemma 3.6, we have that $(d_i^0)^* d_j^0 = 0$ for any $i \neq j$. It follows that

$$\Delta_N^0 = (d^0)^* d^0 = (\bigoplus_{i=1}^{N} d_i^0)^* \bigoplus_{i=1}^{N} d_i^0 = \bigoplus_{i=1}^{N} \bigoplus_{j=1}^{N} (d_i^0)^* d_j^0 = \bigoplus_{i=1}^{N} (d_i^0)^* d_i^0.$$

The desired result follows. □

Theorem 3.8. *Let $G = (V, E)$ be a digraph. The representation matrix of $\Delta_{N,0}^0$ is given by $\sum_{i=1}^{N} L_{N,i}^0$, where $L_{N,i}^0 = (x_{rs})_{1 \leq r,s \leq |V|}$ is defined by*

$$x_{rs} = \begin{cases} \deg_i(v_r), & \text{if } r = s, \\ -n_{rs}, & \text{otherwise.} \end{cases}$$

Here, $\deg_i(v)$ denotes the number of paths of length i that either begin from or end at v, and n_{rs} represents the number of paths of length i between v_r and v_s.

Proof. Let $\gamma_1, \ldots, \gamma_{k_i}$ be the basis of $\Omega_i(G)$. Note that the image of

$$d_i^0 : \Omega_i(G) \to \mathrm{Hom}(\Omega_i(G), \Omega_i(G))$$

contracts to the space generated by $\gamma_1 \cdot \gamma_1^\sharp, \ldots, \gamma_{k_i} \cdot \gamma_{k_i}^\sharp$. Thus the representation matrix of d_i^0 is given by

$$d_i^0 \begin{pmatrix} v_1 \\ \vdots \\ v_k \end{pmatrix} = D_i \begin{pmatrix} \gamma_1 \cdot \gamma_1^\sharp \\ \vdots \\ \gamma_{k_i} \cdot \gamma_{k_i}^\sharp \end{pmatrix},$$

where $v_1, \ldots, v_k$ is the basis of $\Omega_i(G)$, and $D_i = (a_{rs})_{1 \leq r \leq k, 1 \leq s \leq k_i}$ is given by

$$a_{rs} = \begin{cases} 1, & \gamma_s \text{ ends at } v_r; \\ -1, & \gamma_s \text{ begins from } v_r; \\ 0, & \text{otherwise.} \end{cases}$$

It is worth noting that for a path γ that both starts and ends at v, we have $d_i^0(v)(\gamma) = 0$. Thus, the representation of $\Delta_{N,i}^0$ is given by $D_i D_i^T = (x_{rs})_{1 \leq r,s \leq k}$, where

$$x_{rs} = \begin{cases} \deg_i(v_r), & \text{if } r = s, \\ -n_{rs}, & \text{otherwise,} \end{cases}$$

where $\deg_i(v)$ is the number of paths of length i that either begin or end at v, and n_{rs} is the number of paths of length i between v_r and v_s. The desired result follows from Proposition 3.7. □

The computation of the combinatorial Laplacian is generally more complex compared to the graph Laplacian. The graph Laplacian is computationally the least expensive, as it primarily involves operations on adjacency or degree matrices, which are typically of size $n \times n$, where n is the number of vertices. In contrast, the combinatorial Laplacian requires more computational resources due to

the need for higher-dimensional boundary operators and larger matrices associated with simplicial complexes. The size of these matrices depends on the number of k-simplices, which can grow significantly in higher dimensions. The Hochschild Laplacian involves even higher-order algebraic operations, leading to larger and more complex matrices. However, we have developed results such as Theorem 3.5, Proposition 3.7, and Theorem 3.8, which offer efficient methods for computing the Hochschild Laplacian in certain special cases. These results enable our computational approach to achieve efficiency comparable to that of the graph Laplacian and combinatorial Laplacian.

For the Hochschild Laplacian in dimensions larger than 0, it is also possible to compute explicit examples. Below, we provide a simple example to demonstrate the computation process.

Example 3.2. *Let us consider the digraph $G = (V, E)$ from Example 2.2. Note that $\Omega(G) = \mathbb{K}[x]$ is a polynomial algebra, and the Hochschild cohomology in this case is infinite-dimensional. To simplify, we consider the truncated algebra $\Omega_{\leq 1}(G) = \mathbb{K}\{1, x\}$ with the relation $x^2 = 0$. This results in the following cochain complex:*

$$0 \longrightarrow \mathbb{K}\{1,x\} \xrightarrow{d^0} \mathrm{Hom}(\mathbb{K}\{1,x\}, \mathbb{K}\{1,x\}) \xrightarrow{d^1} \mathrm{Hom}(\mathbb{K}\{1,x\} \otimes \mathbb{K}\{1,x\}, \mathbb{K}\{1,x\}) \xrightarrow{d^2} \cdots.$$

Now, consider the linear maps $\delta_1, \delta_x : \mathbb{K}\{1, x\} \to \mathbb{K}\{1, x\}$ defined as follows:

$$\delta_1(a) = \begin{cases} 1, & \text{if } a = 1; \\ 0, & \text{if } a = x; \end{cases} \qquad \delta_x(a) = \begin{cases} 0, & \text{if } a = 1; \\ 1, & \text{if } a = x. \end{cases}$$

It is worth noting that the space $\mathrm{Hom}(\mathbb{K}\{1, x\}, \mathbb{K}\{1, x\})$ is a $\mathbb{K}$-linear space spanned by the four elements $\delta_1, \delta_x, x\delta_1, x\delta_x$, which are mutually orthogonal. Here, the actions of $x\delta_1$ and $x\delta_x$ are given by $(x\delta_1)(a) = x\delta_1(a)$ and $(x\delta_x)(a) = x\delta_x(a)$, respectively. On the other hand, consider the linear maps $\omega_{11}, \omega_{1x}, \omega_{x1}, \omega_{xx} : \mathbb{K}\{1, x\} \otimes \mathbb{K}\{1, x\} \to \mathbb{K}\{1, x\}$ defined as follows:

$$\begin{aligned} \omega_{11}(a \otimes b) &= \delta_1(a)\delta_1(b), \quad & \omega_{1x}(a \otimes b) &= \delta_1(a)\delta_x(b), \\ \omega_{x1}(a \otimes b) &= \delta_x(a)\delta_1(b), \quad & \omega_{xx}(a \otimes b) &= \delta_x(a)\delta_x(b). \end{aligned}$$

The space $\mathrm{Hom}(\mathbb{K}\{1, x\} \otimes \mathbb{K}\{1, x\}, \mathbb{K}\{1, x\})$ is spanned by the following mutually orthogonal elements:

$$\omega_{11}, \omega_{1x}, \omega_{x1}, \omega_{xx}, x\omega_{11}, x\omega_{1x}, x\omega_{x1}, x\omega_{xx}.$$

Here, the action of $x\omega_{uv}$ for $u, v \in \{1, x\}$ is defined by

$$(x\omega_{uv})(a \otimes b) = x\omega_{uv}(a \otimes b).$$

Now, by definition, we have

$$d^1(\delta_1)(a \otimes b) = a\delta_1(b) + \delta_1(a)b - \delta_1(ab).$$

It follows that

$$d^1(\delta_1)(a \otimes b) = \begin{cases} 1, & \text{if } a = b = 1; \\ x, & \text{if } a = 1, b = x; \\ x, & \text{if } a = x, b = 1; \\ 0, & \text{if } a = b = x. \end{cases}$$

Thus, we obtain:

$$d^1(\delta_1) = \omega_{11} + x\omega_{1x} + x\omega_{x1}.$$

Similar calculations yield

$$\begin{aligned} d^1(\delta_x) &= 2x\omega_{xx}, \\ d^1(x\delta_1) &= x\omega_{11}, \\ d^1(x\delta_x) &= 0. \end{aligned}$$

Thus, we can express the action of d^1 in matrix form as

$$d^1 \begin{pmatrix} \delta_1 \\ \delta_x \\ x\delta_1 \\ x\delta_x \end{pmatrix} = \begin{pmatrix} 1 & 0 & 0 & 0 & 0 & 1 & 1 & 0 \\ 0 & 0 & 0 & 0 & 0 & 0 & 0 & 2 \\ 0 & 0 & 0 & 0 & 1 & 0 & 0 & 0 \\ 0 & 0 & 0 & 0 & 0 & 0 & 0 & 0 \end{pmatrix} \begin{pmatrix} \omega_{11} \\ \omega_{1x} \\ \omega_{x1} \\ \omega_{xx} \\ x\omega_{11} \\ x\omega_{1x} \\ x\omega_{x1} \\ x\omega_{xx} \end{pmatrix}.$$

Note that $d^0 = 0$ on $\mathbb{K}\{1, x\}$. It follows that the representation matrix of the Laplacian $\Delta_1^1 : \mathrm{Hom}(\mathbb{K}\{1, x\}, \mathbb{K}\{1, x\}) \to \mathrm{Hom}(\mathbb{K}\{1, x\}, \mathbb{K}\{1, x\})$ is

$$\begin{pmatrix} 3 & 0 & 0 & 0 \\ 0 & 4 & 0 & 0 \\ 0 & 0 & 1 & 0 \\ 0 & 0 & 0 & 0 \end{pmatrix}.$$

The corresponding spectrum is $\mathbf{Spectra}(\Delta_1^1) = \{0, 1, 3, 4\}$.

3.4. Multi-scale Hochschild spectra

A *filtration of digraphs* is a family of digraphs $\{G_\varepsilon\}_{\varepsilon\in\mathbb{R}}$ parameterized by a variable $\varepsilon \in \mathbb{R}$, such that for any $\varepsilon \leq \varepsilon'$, the digraph G_ε is a subgraph of $G_{\varepsilon'}$. More precisely, for any real numbers $\varepsilon_0 \leq \varepsilon_1 \leq \cdots \leq \varepsilon_m$, there exists a sequence of digraphs

$$G_{\varepsilon_0} \hookrightarrow G_{\varepsilon_1} \hookrightarrow \cdots \hookrightarrow G_{\varepsilon_m}.$$

This filtration of digraphs captures the multi-scale structure of the digraph.

Let G be a digraph embedded in Euclidean space, meaning that the vertices of the digraph are points in Euclidean space and the edges are line segments. We define a function $\ell : E \to \mathbb{R}$ by $\ell(e) = \|e\|_2$, where $\|\cdot\|_2$ denotes the L^2-norm. For any real number ε, we define the set $E_\varepsilon = \{e \in E \mid \ell(e) \leq \varepsilon\}$. This gives rise to the subgraph $G_\varepsilon = (V, E_\varepsilon)$ of G. It is clear that the sequence of digraphs $\{G_\varepsilon\}_{\varepsilon\in\mathbb{R}}$ forms a filtration.

Given a digraph G, recall that the number of zero eigenvalues of the Hochschild Laplacian $\Delta_N^n : C^n(\Omega_N(G)) \to C^n(\Omega_N(G))$ equals the Betti number of the corresponding Hochschild homology

$HH^n(\Omega_N(G))$ (Theorem 3.4). The number of zero eigenvalues of the Hochschild Laplacian corresponds to the harmonic feature. Furthermore, the non-zero eigenvalues of the Hochschild Laplacian Δ^n reflect its non-harmonic information. Specifically, the harmonic part refers to the component that corresponds to the most stable or long-lasting features of the graph structure, often capturing the core topological structure. The non-harmonic part, on the other hand, represents more transient features, highlighting the finer details and variations that are not captured by the harmonic part. In particular, the smallest non-zero eigenvalue is a crucial non-harmonic feature and serves as a key geometric characteristic in our applications.

Let $\{G_\varepsilon\}_{\varepsilon\in\mathbb{R}}$ be a filtration of digraphs. Fix an integer $N \geq 0$. We can define the function $\beta^n_{H,N} : \mathbb{R} \to \mathbb{R}$ given by $\beta^n_{H,N}(\varepsilon) = \beta^n_{H,N}(\Omega_{\leq N}(G_\varepsilon))$ for each $n \geq 0$. This function provides a Betti number for each scale, characterizing the multi-scale topological information of the filtration of digraphs. Additionally, we can consider the smallest non-zero eigenvalue of the Hochschild Laplacian to define the function $\lambda^n_{H,N} : \mathbb{R} \to \mathbb{R}$, given by the smallest non-zero eigenvalue of the Hochschild Laplacian Δ^n_N on G_ε for each $n \geq 0$. The two functions $\beta^n_{H,N}$ and $\lambda^n_{H,N}$ are the main topological features we develop in this work for data analysis. For computational convenience, the functions $\beta^0_{H,N}$ and $\lambda^0_{H,N}$, or more specifically, the functions $\beta^{0,i}_{H,N}$ and $\lambda^{0,i}_{H,N}$, are used to compute Hochschild features. Here, $\lambda^{0,i}_{H,N}$ denotes the smallest nonzero eigenvalue of the Laplacian component $\Delta^0_{N,i}$.

Example 3.3. *Consider the finite set of points X in the Euclidean plane given by*

$$P_1\,(0,1)\,,\ P_2\left(\frac{\sqrt{3}}{2},\frac{1}{2}\right),\ P_3\left(\frac{\sqrt{3}}{2},-\frac{1}{2}\right),\ P_4\,(0,-1)\,,\ P_5\left(-\frac{\sqrt{3}}{2},-\frac{1}{2}\right),\ P_6\left(-\frac{\sqrt{3}}{2},\frac{1}{2}\right).$$

The digraph G is given in Example 3.3. Note that the algebra $\Omega(G)$ is infinite-dimensional. We consider the truncated algebra $\Omega_{\leq 2}(G)$. The filtration parameter changes at the values $\varepsilon = 1$ and $\varepsilon = \sqrt{3}$. By a direct calculation, the representation matrix of $\Delta^0_{N,0}$ at $\varepsilon = 1$ is given by

$$\begin{pmatrix} 4 & -1 & -1 & 0 & -1 & -1 \\ -1 & 4 & -1 & -1 & 0 & -1 \\ -1 & -1 & 4 & -1 & -1 & 0 \\ 0 & -1 & -1 & 4 & -1 & -1 \\ -1 & 0 & -1 & -1 & 4 & -1 \\ -1 & -1 & 0 & -1 & -1 & 4 \end{pmatrix}.$$

The spectra of $\Delta^0_{N,0}$ is given by

$$\mathbf{Spectra}(\Delta^0_{N,0}) = \{0, 4, 4, 4, 6, 6\}.$$

Similarly, we can obtain the spectra of $\Delta^0_{N,1}$ as follows:

$$\mathbf{Spectra}(\Delta^0_{N,1}) = \{0.693, 12, 12, 12, 17.307, 18\}.$$

Thus, we obtain the functions $\beta^{0,0}_{H,2}$ and $\lambda^{0,0}_{H,2}$, as shown in Figure 1. The simplicity of the curves is due to the high symmetry of the digraph in this example. For more complex structural applications, we can observe greater variability in the functions.

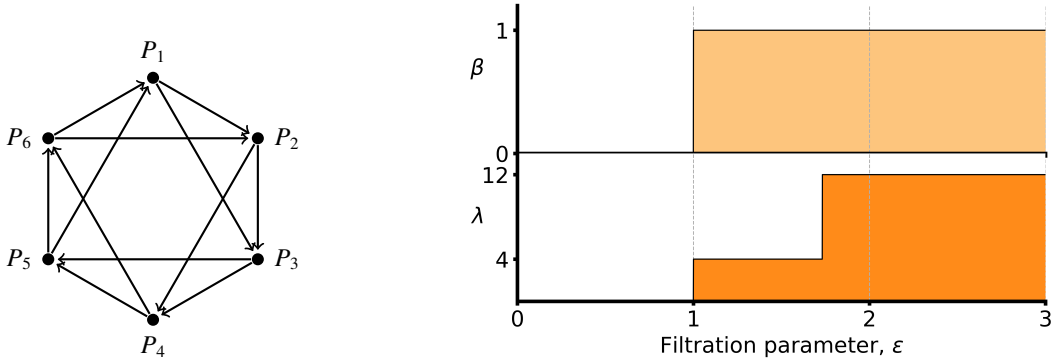

Figure 1. The left figure is the digraph in the Euclidean plane in Example 3.3, and the right figure shows the functions $\beta_{H,2}^{0,0}$ and $\lambda_{H,2}^{0,0}$ that represent the Hochschild topological features.

3.5. Comparison with persistent homology and multi-scale graph spectra

To further highlight the strengths of the multi-scale Hochschild spectra, we provide a comparative analysis with traditional persistent homology and multi-scale graph spectra approaches across three key aspects: directed edge support, topological and geometric information, and high-dimensional information, as summarized in Table 1.

Table 1. Comparative analysis of persistent homology, graph Laplacian, and multi-scale Hochschild spectra

Aspect	Persistent Homology	Multi-scale Graph Spectra	Multi-scale Hochschild Spectra
Directed Edge Support	Not supported	Undirected graphs	Supports directed edges
Topological and Geometric Information	Harmonic only	Harmonic and non-harmonic	Harmonic and non-harmonic (via multi-scale Hochschild spectras)
High-Dimensional Information	Supports high dimensions	Limited to 0th and 1st dimensions	Supports high dimensions

First, in terms of directed edge support, traditional persistent homology relies on simplicial complexes such as Vietoris-Rips and Čech complexes, which are primarily designed for point clouds and undirected graphs. As a result, they cannot represent directed edges, making them unsuitable for digraph analysis. Similarly, the multi-scale graph spectra is defined for undirected graphs and fails to account for edge directionality. In contrast, the multi-scale Hochschild spectra leverages Hochschild cohomology, enabling the direct incorporation of directed edges into the analysis. This makes it particularly effective for studying digraph data.

Second, regarding topological and geometric information, traditional persistent homology exclusively captures harmonic information, focusing on stable topological features while neglecting non-harmonic components. On the other hand, the multi-scale graph spectra combines both harmonic and non-harmonic information, offering insights into the spectral and geometric properties of undirected graphs. The multi-scale Hochschild spectra advances this further by integrating both harmonic and non-harmonic information within the framework of Hochschild cohomology. This integration allows for a richer characterization of the topological and geometric features of digraphs, making it highly suitable for analyzing complex directed networks.

Finally, when considering high-dimensional information, the multi-scale graph spectra is restricted to the 0th and 1st dimensions, limiting its applicability to higher-dimensional analysis. In contrast, the persistent homology and multi-scale Hochschild spectra support high-dimensional analysis by utilizing truncated path algebras, balancing computational efficiency with the ability to extract complex

topological features.

These comparisons demonstrate the unique advantages of the multi-scale Hochschild spectra over traditional approaches, particularly in its capacity to handle directed edges, integrate harmonic and non-harmonic information, and efficiently analyze high-dimensional structures.

4. Applications

In the previous sections, we explore Hochschild cohomology of path algebra and multi-scale Hochschild spectra. The harmonic information provided by the multi-scale Hochschild spectra is reflected in the Betti numbers, while its non-harmonic information is captured by the positive eigenvalues. In this section, our main work is to demonstrate how to extract Hochschild characteristics from the three-dimensional structure of molecules. We will not perform a deeper analysis of these Hochschild characteristics in this work, as there are many powerful methods for analyzing topological features, including deep learning and natural language models [11].

In this work, we will consider two of the most common drugs: ibuprofen ($C_{13}H_{18}O_2$) and aspirin ($C_9H_8O_4$). Ibuprofen is a nonsteroidal anti-inflammatory drug (NSAID) commonly used to reduce pain, fever, and inflammation in conditions such as headaches and arthritis. Aspirin, also an NSAID, is used to relieve pain and inflammation and, in low doses, helps reduce the risk of heart attacks and strokes due to its blood-thinning effects.

As shown in Figure 3(a), green balls represent hydrogen atoms, brown balls represent carbon atoms, and blue balls represent oxygen atoms. Based on the electronegativities of these atoms, carbon: 2.55, hydrogen: 2.20, and oxygen: 3.44, we can determine the directed edges in the graph, with the direction always pointing from the atom with lower electronegativity to the atom with higher electronegativity. For any filtration parameter ε, we connect atoms within a distance of ε with directed edges, resulting in a digraph. As the filtration parameter increases, we obtain a filtration of digraphs. Subsequently, we compute the Hochschild cohomology and Hochschild Laplacian to obtain the Hochschild Betti number $\beta^{0,0}_{H,N}$ and the smallest positive eigenvalue $\lambda^{0,0}_{H,N}$. Here, we typically use $N = 2$, indicating the use of the 2-truncated path algebra.

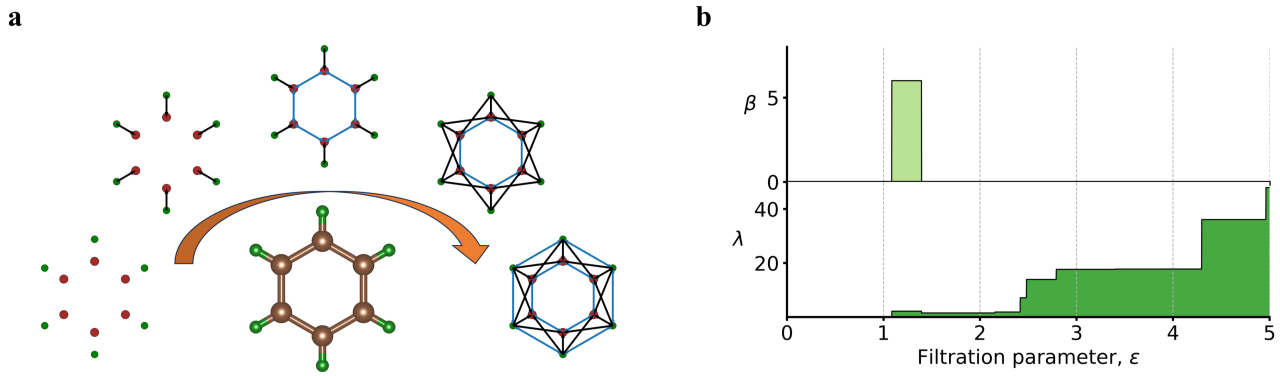

Figure 2. (a) The graphical representation of benzene and the filtration of digraphs derived from the benzene structure; (b) the Hochschild Betti number $\beta^{0,0}_{H,2}$ of aspirin and the Hochschild smallest positive eigenvalue $\lambda^{0,0}_{H,2}$ of benzene.

As shown in Figure 2(a), the benzene molecule, composed of 6 carbon atoms and 6 hydrogen atoms,

develops directed edges between atoms as the filtration parameter increases. At a parameter value of approximately 1.086 Å, directed edges from hydrogen atoms to carbon atoms appear. At around 1.395 Å, two directed edges emerge between each pair of adjacent carbon atoms, pointing to various carbon atoms. At approximately 2.154 Å, six new directed edges from hydrogen atoms to carbon atoms are formed. This process continues, resulting in a filtration of digraphs. Figure 2(b) shows the variation of the Hochschild Betti number and the smallest positive eigenvalue for benzene.

For ibuprofen and aspirin, we can similarly obtain their corresponding filtrations of digraphs, analogous to the treatment of the benzene structure, and compute their Hochschild topological features. Figures 3(a) and (b) provide graphical representations of ibuprofen and aspirin, respectively. Figures 3(c) and (d) show the Hochschild topological features for ibuprofen and aspirin, namely the Hochschild Betti number $\beta^{0,0}_{H,2}$ and the smallest positive eigenvalue $\lambda^{0,0}_{H,2}$. For more general values of N, our calculations follow a similar approach; however, computations for higher-dimensional Laplacians become more complex. Therefore, the algorithm still has potential for improvement.

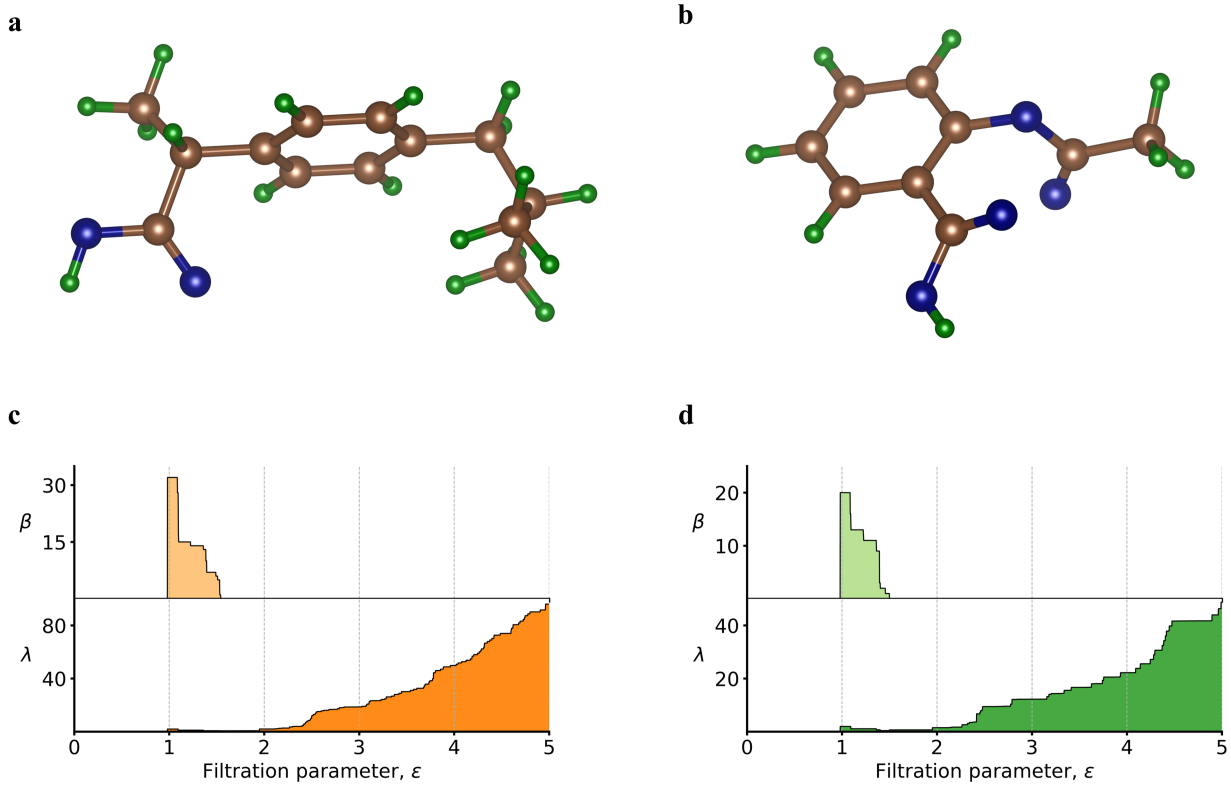

Figure 3. (a) The graphical representation of ibuprofen; (b) the graphical representation of aspirin; (c) the Hochschild Betti number $\beta^{0,0}_{H,2}$ of ibuprofen and the Hochschild smallest positive eigenvalue $\lambda^{0,0}_{H,2}$ of ibuprofen; (d) the Hochschild Betti number $\beta^{0,0}_{H,2}$ of aspirin and the Hochschild smallest positive eigenvalue $\lambda^{0,0}_{H,2}$ of aspirin.

In our computations, we calculated the filtration parameter from 0 to its maximum value, which ensures that any two points are connected. The filtration range shown in Figures 2 and 3 is chosen from 0 to 5 Å to highlight the variations in Betti numbers, which are primarily observed within the 1–1.5 Å range. The computational cost for calculating the Hochschild spectra for ibuprofen and aspirin

is approximately 2.05 seconds and 0.38 seconds, respectively. These computations were performed on a personal laptop equipped with an AMD Ryzen 5 5600H processor, Radeon Graphics, and 16 GB of RAM. We believe these computation times are reasonable for larger datasets and can be further optimized when executed on a dedicated server with higher computational resources.

5. Conclusions

The development of topological data analysis has become increasingly advanced, with a growing array of topological and geometric methods being explored. It is challenging to determine the absolute effectiveness of these methods, as their performance can vary depending on the dataset and application context. Generally, a method is considered effective if it meets at least two criteria: first, it should have a suitable framework for modeling the dataset; second, it should ensure computational efficiency. The multiscale Hochschild spectral analysis developed in this work meets both of these criteria. This method is applicable to digraph data and can even model certain weighted point cloud data. Additionally, the corresponding Hochschild spectral information is relatively straightforward to compute.

In this work, we introduce the Hochschild Laplacians for digraphs and propose a Hochschild spectral analysis for digraph data. Compared to the classical spectral analysis of graphs, Hochschild spectral analysis offers a new perspective based on a different mathematical theory. We begin by providing an overview of Hochschild cohomology and path algebras for digraphs. For digraphs with directed cycles, the path algebra is infinite-dimensional, as shown in Proposition 2.2. To address this, we consider truncated path algebras, which are finite-dimensional. We present some interesting results on truncated path algebras, such as the relationship between the 1st Hochschild Betti number and the Euler characteristic of the digraph, as discussed in Theorem 3.3. Additionally, we introduce the Hochschild Laplacian, whose harmonic spectral information aligns with Hochschild cohomology, as stated in Theorem 3.4, while its non-harmonic components provide further geometric insights. We also compute the matrix representation of the Hochschild Laplacian and find connections between this matrix and the classical graph Laplacian, with details provided in Section 3.3. Furthermore, we define and compute the multiscale Hochschild spectra. Finally, we apply this method to calculate the Hochschild Betti numbers and the smallest positive eigenvalue for common drug molecules such as ibuprofen and aspirin, which serve as visualizable topological features. The proposed framework not only extends Hochschild cohomology to a practical tool for digraph analysis but also achieves a balance between computational feasibility and the richness of extracted features, demonstrating its potential in both theoretical and applied domains.

This work introduces a novel method for processing graph data; however, it has certain limitations that require further refinement. From a theoretical perspective, extending Hochschild cohomology into a persistent cohomology framework remains challenging, largely because Hochschild cohomology is not functorial with respect to path algebras. In terms of applications, while we have demonstrated the potential of Hochschild spectral analysis in extracting features of molecular structures, its application to concrete datasets through topological feature analysis remains underdeveloped. Future research will address these challenges. Additionally, we focus on further optimization of computational methods for handling large-scale digraphs. Moreover, integrating the multi-scale Hochschild spectra with machine learning models for feature extraction and prediction opens new possibilities for interdisciplinary

applications, bridging topology and data-driven approaches. Consequently, there is significant scope for further exploration of Hochschild spectral analysis, and we anticipate that it will provide valuable insights in both theoretical and applied topology.

Author contributions

Yunan He: Formal analysis, Created visualizations, Validated results, Writing–original draft. Jian Liu: Designed project, Writing–original draft, Writing–review and editing. All authors have read and approved the final version of the manuscript for publication.

Use of Generative-AI tools declaration

The authors declare that they have not used Artificial Intelligence (AI) tools in the creation of this article.

Acknowledgments

This work was supported in part by the Natural Science Foundation of China (NSFC) grant (12401080), and the Natural Science Foundation of Chongqing, China (CSTB2024NSCQ-LZX0136).

Conflict of interest

The authors declare that there is no conflict of interest.

References

1. Y. Ahamad, U. Ali, I. Siddique, A. Iampan, W. A. Afifi, H. A. Khalifa, Computing the normalized Laplacian spectrum and spanning tree of the strong prism of octagonal network, *J. Math.*, **2022** (2022), 9269830. https://doi.org/10.1155/2022/9269830
2. P. Bendich, J. Harer, Persistent intersection homology, *Found. Comput. Math.*, **11** (2011), 305–336. https://doi.org/10.1007/s10208-010-9081-1
3. W. Y. Bi, J. Y. Li, J. Liu, J. Wu, On the Cayley-persistence algebra, 2022, arXiv:2205.10796.
4. Z. X. Cang, L. Mu, K. D. Wu, K. Opron, K. L. Xia, G.-W. Wei, A topological approach for protein classification, *Mol. Based Math. Biol.*, **3** (2015), 140–162. https://doi.org/10.1515/mlbmb-2015-0009
5. L. Caputi, H. Riihimäki, Hochschild homology, and a persistent approach via connectivity digraphs, *J. Appl. and Comput. Topology*, **8** (2024), 1121–1170. https://doi.org/10.1007/s41468-023-00118-9
6. G. Carlsson, Topology and data, *Bull. Amer. Math. Soc.*, **46** (2009), 255–308. https://doi.org/10.1090/S0273-0979-09-01249-x
7. G. Carlsson, V. De Silva, Zigzag persistence, *Found. Comput. Math.*, **10** (2010), 367–405. https://doi.org/10.1007/s10208-010-9066-0

8. G. Carlsson, T. Ishkhanov, V. De Silva, A. Zomorodian, On the local behavior of spaces of natural images, *Int. J. Comput. Vis.*, **76** (2008), 1–12. https://doi.org/10.1007/s11263-007-0056-x
9. G. Carlsson, G. Singh, A. Zomorodian, Computing multidimensional persistence, In: *Algorithms and computation*, Heidelberg: Springer, 2009, 730–739. https://doi.org/10.1007/978-3-642-10631-6_74
10. G. Carlsson, A. Zomorodian, The theory of multidimensional persistence, *Discrete Comput. Geom.*, **42** (2009), 71–93. https://doi.org/10.1007/s00454-009-9176-0
11. D. Chen, J. Liu, G.-W. Wei, Multiscale topology-enabled structure-to-sequence transformer for protein–ligand interaction predictions, *Nat. Mach. Intell.*, **6** (2024), 799–810. https://doi.org/10.1038/s42256-024-00855-1
12. D. Chen, J. Liu, J. Wu, G.-W. Wei, Persistent hyperdigraph homology and persistent hyperdigraph Laplacians, *Found. Data Sci.*, **5** (2023), 558–588. https://doi.org/10.3934/fods.2023010
13. J. H. Chen, R. D. Zhao, Y. Y. Tong, G.-W. Wei, Evolutionary de Rham-Hodge method, *Discrete Cont. Dyn.-B*, **26** (2021), 3785–3821. https://doi.org/10.3934/dcdsb.2020257
14. S. Chowdhury, F. Mémoli, Persistent path homology of directed networks, In: *Proceedings of the twenty-ninth annual ACM-SIAM symposium on discrete algorithms*, 2018, 1152–1169. https://doi.org/10.1137/1.9781611975031.75
15. J. R. Clough, N. Byrne, I. Oksuz, V. A. Zimmer, J. A. Schnabel, A. P. King, A topological loss function for deep-learning based image segmentation using persistent homology, *IEEE T. Pattern Anal.*, **44** (2020), 8766–8778. https://doi.org/10.1109/TPAMI.2020.3013679
16. V. De Silva, D. Morozov, M. Vejdemo-Johansson, Persistent cohomology and circular coordinates, *Discrete Comput. Geom.*, **45** (2011), 737–759. https://doi.org/10.1007/s00454-011-9344-x
17. H. Derksen, J. Weyman, Quiver representations, *Notices of the AMS*, **52** (2005), 200–206.
18. H. Edelsbrunner, D. Letscher, A. Zomorodian, Topological persistence and simplification, *Discrete Comput. Geom.*, **28** (2002), 511–533. https://doi.org/10.1007/s00454-002-2885-2
19. M. Gerstenhaber, S. D. Schack, Simplicial cohomology is Hochschild cohomology, *J. Pure Appl. Algebra*, **30** (1983), 143–156. https://doi.org/10.1016/0022-4049(83)90051-8
20. N. Giansiracusa, R. Giansiracusa, C. Moon, Persistent homology machine learning for fingerprint classification, *2019 18th IEEE International Conference on Machine Learning and Applications (ICMLA)*, Boca Raton, FL, USA, 2019, 1219–1226. https://doi.org/10.1109/ICMLA.2019.00201
21. G. Hochschild, On the cohomology groups of an associative algebra, *Ann. Math.*, **46** (1945), 58–67. https://doi.org/10.2307/1969145
22. Y. Jiang, D. Chen, X. Chen, T. Y. Li, G.-W. Wei, F. Pan, Topological representations of crystalline compounds for the machine-learning prediction of materials properties, *npj Comput. Mater.*, **7** (2021), 28. https://doi.org/10.1038/s41524-021-00493-w
23. J. Liu, D. Chen, F. Pan, J. Wu, Neighborhood path complex for the quantitative analysis of the structure and stability of carboranes, *J. Comput. Biophys. Che.*, **22** (2023), 503–511. https://doi.org/10.1142/S2737416523500229

24. J. Liu, D. Chen, G.-W. Wei, Persistent interaction topology in data analysis, 2024, arXiv:2404.11799.

25. J. Liu, J. Y. Li, J. Wu, The algebraic stability for persistent Laplacians, *Homol. Homotopy Appl.*, **26** (2024), 297–323. https://dx.doi.org/10.4310/HHA.2024.v26.n2.a15

26. X. Liu, X. J. Wang, J. Wu, K. L. Xia, Hypergraph-based persistent cohomology (HPC) for molecular representations in drug design, *Brief. Bioinform.*, **22** (2021), bbaa411. https://doi.org/10.1093/bib/bbaa411

27. U. Lupo, A. M. Medina-Mardones, G. Tauzin, Persistence Steenrod modules, *J. Appl. and Comput. Topology*, **6** (2022), 475–502. https://doi.org/10.1007/s41468-022-00093-7

28. C. S. Pun, S. X. Lee, K. L. Xia, Persistent-homology-based machine learning: a survey and a comparative study, *Artif. Intell. Rev.*, **55** (2022), 5169–5213. https://doi.org/10.1007/s10462-022-10146-z

29. R. Wang, D. D. Nguyen, G.-W. Wei, Persistent spectral graph, *Int. J. Numer. Meth. Bio.*, **36** (2020), e3376. https://doi.org/10.1002/cnm.3376

30. K. L. Xia, G.-W. Wei, Persistent homology analysis of protein structure, flexibility, and folding, *Int. J. Numer. Meth. Bio.*, **30** (2014), 814–844. https://doi.org/10.1002/cnm.2655

AIMS Press